Check for updates

DOI: 10.1002/ admt.201800334

Article type: Full Paper

Title: Selective oxidation and carbonization by laser writing into porous silicon

Adrian Keating and Xiao Sun*

A. Keating, Ass/Prof.

Microelectronics Research Group

Department of Mechanical Engineering, Mail Bag M050

School of Engineering,

The University of Western Australia,

35 Stirling Hwy, 6009, CRAWLEY, Western Australia

E-mail: adrian.keating@uwa.edu.au

X. Sun, Research Associate

Microelectronics Research Group

Department of Electrical, Electronic and Computer Engineering,
School of Engineering,

The University of Western Australia,

35 Stirling Hwy, 6009, CRAWLEY, Western Australia

Author Manuscript

This is the author manuscript accepted for publication and has undergone full peer review but has not been through the copyediting, typesetting, pagination and proofreading process, which may lead to differences between this version and the Version of Record. Please cite this article as doi: 10.1002/admt.201800334.

This article is protected by copyright. All rights reserved.

Keywords: porous silicon, carbonization, oxidation, laser-writing, laser-induced

Author Manuscript

Abstract: We demonstrate the selective formation of either oxidized or carbonized features into 2.5-μm thick porous silicon films using laser writing at a wavelength of 405 nm. Oxidized features are formed in air while carbonized features are achieved during the flow of propane at 600 sccm. Voids which have been previously associated with the use of propane are not observed, largely due to the rapid heating and high flow rates achieved in the experiment. Carbonized regions with feature widths down to 1.8 μm are achieved and chemical resistance to both HF and KOH is demonstrated. Once carbonized regions are formed, the surrounding areas can be overwritten in air to convert the surrounding regions into oxidized porous silicon allowing films to be created with as-fabricated, oxidized and carbonized regions. Energy dispersive X-Ray and Raman analysis confirms the presence of carbon within the written structures. At high optical powers, cracking around the carbonized features is observed which is attributed to a contraction of the film. Such cracking is not observed during selective oxidation of features. This work significantly enhances the ability to engineer and pattern the composition of porous silicon films enabling selective control of the material's properties and functionality.

1. Introduction: Porous silicon films containing nano-size pores provide a platform to create highly sensitive sensors which can leverage the extremely large surface area of the films. For example, the optical properties of waveguides[1] and gratings[2, 3] undergo significant change as a result of gas or vapour penetration into the pores, while bio-sensing through electrical or optical methods is enhanced by the large adsorption surface.[4] By combining this large detection area with complex waveguide interferometers, a limit of detection of 10^{-5} refractive index units has been achieved.[5] However the as-fabricated hydrogenated surface chemistry of porous silicon has a high reactivity leading to dissolution in mildly alkaline solutions as well as changes in the film characteristics over time.[6] The need for stable films has driven the development of passivation technologies via oxidation,[7] nitridation[6] or carbonisation[8] typically at annealing temperatures of

This article is protected by copyright. All rights reserved.

at least 600 °C. These passivation techniques can also allow microelectronic photolithographic processes to be used to form the microscale features required for complex sensors[9], however the high passivation temperatures limit the order in which the fabrication processes can be applied.[10]

Beyond photolithography, patterning of microscale features in porous silicon has been demonstrated with various approaches including imprinting[3], e-beam lithography[11] and laser writing. [1, 5, 12, 13] Creating features via laser writing in porous silicon is particularly useful as the localised high temperatures can simultaneously create microscale features and passivate the films through oxidation. The selectively oxidized features are stable and allow modulation of the refractive index to create structures such as diffraction gratings,[12] however the volume expansion of the SiO_2 leads to compressive stress, swelling and pore closure.[14] The closed pores degrade the key advantage of large surface area in the films and stress affects opportunities to develop micro-electro-mechanical systems (MEMS) based sensors.[15] As a result, once the laser written oxidized features are created, they are typically removed through hydrofluoric (HF) acid immersion. The features that remain after oxide removal define the regions of interest,[5, 12, 13] but form a negative of the original (exposed) design and any localised passivation in the composition of the film resulting from laser writing is not inherited by the final device, leaving an unstable, reactive surface.

There has been intense interest in the use of carbonization to passivate porous silicon films. Carbonization can be achieved through a number of wet and gas-based processes,[16] with the use of acetylene at 600 °C being the most widely used approach for carbonization of an entire film. The carbonization process ensures the pores remain open and clear, maintaining the large surface after thermal treatment. Much of the original work investigating the formation of carbon barrier layers and SiC on silicon was based on the use of propane, but the formation of voids under some

Author Manuscript

This article is protected by copyright. All rights reserved.

conditions lead to the use of acetylene.[17, 18] However under high flow rates (>30 sccm) and rapid heating conditions, voids were shown to be absent when using propane to form SiC.[17] To date, no demonstration of the carbonization of porous silicon using propane has been demonstrated.

Recently, porous carbonized features have been created using direct laser writing onto polymer based substrates,[19] where the intense heat generated by the laser is used to form the carbonized regions. The resulting conductive and porous traces[20] can support a range of devices including strain gages[21] and super-capacitors.[22] These advances motivate our interest to form carbonized porous films directly into porous silicon, as a silicon based platform provides a proven path towards mass production. **Table 1** provides a comparison of polymeric and silicon based laser writing approaches, with significantly finer features being produced on silicon based platforms. However, to date, laser writing into porous silicon has only been demonstrated in air, resulting in oxidized features with the associated issues addressed above.

In this work we propose and demonstrate both carbonization of selective regions of porous silicon (PS) films during laser writing and the use of propane as the passivation gas. High flow rates and rapid, localised heating prevented the formation of voids which have previously been associated with the use of propane. Complex features as fine as 1.8 µm have been achieved while maintaining the open nanoscale porous features of the film. By altering gas flows, a combination of surface passivations can be achieved within the same film, providing the ability to modulate the surface passivation within the film. Chemical resistance to both HF and alkaline developer containing potasium hydroxide (KOH) developers is demonstrated with the laser written regions remaining as the features of interest after wet processing (positive masking) to remove the surrounding PS or intentionally oxidized regions. This process may provide a simple path to form patterned, chemically

Author Manuscript

This article is protected by copyright. All rights reserved.

robust sensors with a nanoscale porous structure which can utilize a combination of surface passivations.

2. Methods: The PS was fabricated on moderately doped p-type (100) silicon with resistivity of 0.08-0.12 Ω·cm. Room temperature anodisation was performed in 15% HF/ethanol with a constant current density of 10 mA/cm^2 for 403 seconds in the dark to achieve a physical thickness of 2.5 µm. For the laser writing, a 405 nm laser was focused through a microscope with a 5× objective to achieve a spot size diameter of ∅ = 3 µm. The laser driver circuit adjusted the current through the laser (and hence the power) and was controlled via G-code during writing of complex structures. Data is presented in terms of optical power, beam widths and laser writing speeds (or dwell times) which allows calculation of fluence or power density where required. The sample was housed in a chamber (volume 120×70×30 mm^3) with a glass lid and inlet/outlet feeds for either air or propane injection/venting. Carbonization studies used propane flow rates of 0.6 L/min while selective oxidation was achieved by allowing air to diffuse into the chamber. Where a raster pattern over a large area was required during oxidation, the beam was defocused by the addition of a 300 µm thick glass sheet into optical path after the lens, which produced a consistent increase in the beam diameter to 16 µm. Post laser writing, samples were measured on a Zygo optical profilometer (NewView 6300) after a short immersion in 10% HF:EtOH for 10 s or 1% KOH (AZ326 developer). SEM and EDX measurements were performed on a Verios XHR or a Zeiss 1555 SEM while Raman studies were conducted with a WITec alpha 300RA+. Post image analysis was performed using Gwyddion, ImageJ and Matlab.

3.1 Experimental Results: Gas modulated passivation during laser writing of porous silicon

Author Manuscript

This article is protected by copyright. All rights reserved.

Initially a series of straight lines were written into porous silicon using a raster pattern at a speed of v = 200 μm/s. These laser written passivated features were created with either a propane flow (600 sccm) or ambient air conditions. After HF-immersion to remove oxidized porous silicon, the profile width of each line written at a different power was measured as shown in **Figure 1a**. For each measurement in air, the etch depth reached very close to the substrate depth (2.5 μm), indicating that oxide formed throughout the film where exposed to the laser beam, consistent with previous results.[24] By comparison, under the flow of propane, at powers lower than 377 μW the profiles shown in Figure 1a have only a minor (<500 nm) dip below the surface, suggesting virtually no oxidation occurred, a significant difference from the air-passivated features at the same power. More details of features written at a low power in either air or propane are shown in Figure 1b, indicating very similar profiles but significantly reduced etch depth after HF immersion for the propane exposed sample. At a high power of 1.077 mW shown in Figure 1c, the propane written features were observed to have narrow pits around a central passivated region. These pits were present prior to HF immersion, suggesting damage occurred during laser writing under the flow of propane. As these pits did not appear in the samples passivated in air, we believe the damage in propane exposed samples is due to thermal contraction, suggesting a change in the thermal properties of the films.

It is known that hydrogen desorption from porous silicon occurs at temperatures between 350 °C and 500 °C, and once films are desorbed and exposed to air, considerable oxidation occurs.[15] Similarly, surface carbonization has been observed to be initiated in this range of temperatures under continuous acetylene flow conditions, with complete desorption and gas dissociation occurring at temperatures above 600 °C.[3] As illustrated in **Figure 2a**, we believe at sufficiently high

Author Manuscript

This article is protected by copyright. All rights reserved.

optical powers, the region exposed to the centre of the Gaussian laser beam reaches temperatures of 350 °C or more, while the temperature further from the centre is lower. In the spatial region where the temperature drops below 350 °C, incomplete passivation occurs and the rapid change in material properties over short distances appears to result in large differential stresses (contraction) during propane passivation, resulting in the cracking seen as pits around the exposed region.

Under the same condition as that shown in Figure 1, where all samples were immersed in HF after laser writing, the depth of each etched profile was measured as shown in Figure 2b. The air exposed regions etched down the entire film depth (2.5 μm) at a power of 80 μW (fluence F= 170 mJ/mm^2) after HF immersion, consistent with previously reported measurements.[24] By comparison, above 100 μW our propane exposed films maintained a constant depression depth of 490±40 nm below the surface, a value which was maintained over a wide power range up to 1 mW. This depression below the surface was present before the HF dip and so was not associated with oxidation of the film but suggests a structural rearrangement and in-plane contraction of the film. Above 580 μW, pits down to the Si/PS interface appeared on the outer edge of the exposed regions (shown in Figure 2a), even before samples were dipped in HF. After HF exposure these pits were largely unaffected, however the top surface region was slightly depressed (see Figure 1a at high power) suggesting partial oxidation at the surface.

While useful to show the etch depth, the measurements in Figure 2b provide little information regarding the exposure process once the substrate depth has been reached. To complement this data, we have also analysed the *width* of the post-HF etched profile as shown in Figure 2c on a semi-log-x scale. For the air-passivated features, a logarithmic increase in the width is measured across more than 2-orders of magnitude change in the exposed power. However profile width

Author Manuscript

This article is protected by copyright. All rights reserved.

measurements for the propane exposed samples (attributed to a carbonization hypothesis) were constant at 1.8 µm up to 1 mW. At higher powers (*P*), the measured width is largely independent of the laser beam diameter and a linear extrapolation to the abscissa indicates the threshold power which initiates the thermally driven passivation. The solution to the steady state heat equation in radial coordinates (*r*) for a point heat source from a laser leads to a temperature (*T*) dependence that contains the product of a modified Bessel function and a decaying exponential, both of which depend on *r*.[25] When *r* is large compared to the laser beam width ∅, this gives rise to a spatial temperature profile of the form $T \propto Pe^{-r/r_0}$ so that plotting using *log*(*P*) highlights any linear radial dependence. The width measured in Figure 2c represents the maximum radial distance to achieve the temperature required to initiate the passivation process. By extrapolating the high power measurements, the threshold power for air was found to be $P_{air} = 0.035$ mW while for propane it was $P_{C3H8} = 0.91$ mW. In air this threshold power is consistent with the power required to create deep features as shown in Figure 3b, while for propane this power is associated with the onset of the cracking (pitting) again possibly associated with deep feature formation and the associated stresses. The pit-to-pit width (or pit diameter) was present only in the propane exposed samples and increased above 1 mW. At all power levels, the profile width of the propane exposed samples was less than the air exposed samples. Importantly, under the high flow rates of propane used here and the rapid heating time induced by the laser, no voids were observed in any experiments when using propane, supporting previous observations.[17] Table 1 compares the minimum features sizes achieved in this work with that of other similar studies, showing our results are comparable to the feature sizes achieved in oxidized porous silicon. Figure 2c indicates that carbonized porous features can be achieved which are significantly smaller than the equivalent oxidized features and we believe

Author Manuscript

This article is protected by copyright. All rights reserved.

by using high N.A. objectives, finer sub-micron scale features should be achievable using our approach.

3.2 Experimental Results: Multi-composition surface features via laser writing

As the type of carrier gas provided the ability to switch between selective oxidization or carbonization of the porous silicon, an investigation was undertaken to combine both these features during laser writing. In Step #1, pillars were formed into porous silicon by a single exposure of P=0.83 mW for a dwell time of Δt=100 ms at each point (C_3H_8 600 sccm, $\varnothing$ = 3 µm and v = 0 µm/s). In Step #2, the laser beam diameter was broadened to $\varnothing$ = 16 µm and the power increased to P = 6 mW while a raster pattern was written in air at a speed of v = 50 µm/s over part of the area exposed in Step #1. The increased beam size in Step #2 was chosen to achieve uniform oxidation over a broad area in a reasonable time. The entire sample was then immersed in HF:EtOH for 10 s. **Figure 3a** shows the resulting array of circular carbonized PS-pillars of average diameter 6.3 µm, eccentricity 0.57 and height of 2.2 µm. While semiconductor lasers are known to have astigmatism and an elliptical beam that can lead to such eccentricity, the linear polarisation of the laser may also lead to selective heating along the polarization axis, requiring further study to separate out these effects.[24] The raster pattern produced by the larger area beam in Step #2 had a pitch of 8 µm which can be seen in the background of Figure 3a. Image analysis of the SEM data indicates the pores in the pillar remained open with sizes ranging from 10-70 nm, consistent with the original PS. Figure 3b shows a single pillar in the region shown which had not under gone Step #2 exposure in air. Clear cracking is present in the PS around the pillar showing the source of the pitting measured in Figure 2c. The uniformity of the cracking around the central pillar supports the premise that uniform contraction of the pillar during rapid laser heating in propane has caused the cracking. Tensile stress

Author Manuscript

This article is protected by copyright. All rights reserved.

is consistent with films annealed at temperatures above 600 °C without oxygen present[15] and would result in contraction of the film. In spite of the cracking, there was 100% yield of the carbonized pillars demonstrating a robust and stable surface considering that after formation, pillars had undergone exposure to a high power laser beam in air followed by HF immersion.

Figure 3c shows EDX studies of the pillar shown in Figure 3b, indicating a high carbon content in the 3 µm region in the centre of the pillar. At the periphery of the pillar, the oxygen content increases, to encompass a 6.4 µm diameter, suggesting the region of the pit may also contain oxidized porous silicon which formed after HF immersion of the laser written features once exposed to air. The darker central region on the SEM is suggestive of a more conductive material, consistent with thermally carbonized PS.[26] Silicon content appeared lowest in the central 3 µm region and continues to decrease out to 6 µm. The high silicon content outside of the pillar region is due to the surrounding as-fabricated porous silicon film which contributes most to the background signal. The central silicon content appears lower because the EDX incident electrons only probe the first few hundred nanometers. Outside of the regions exposed in Step #2, the film remains porous silicon, un-oxidized and un-carbonized. Hence prior to HF immersion, the films consisted by 3 different materials – porous silicon, oxidized porous silicon and carbonized porous silicon.

Raman measurements of the film have also been conducted to confirm the presence of carbonized porous silicon. Figure 4 show the scan resulting from the region where the films were carbonized in Step #1 of Figure 3 as well as the regions where the films were oxidized and subsequently stripped of oxide in Step #2. In the region associated with Step #2, a single, narrow strong peak count indicates the presence of silicon, with secondary features supressed by 34:1, indicating a largely silicon rich surface due to the substrate response. In the region which has been carbonized in Step #1, porous

Author Manuscript

This article is protected by copyright. All rights reserved.

silicon remains, indicated by the narrow but supressed (6:1) silicon peak compared to the silicon substrate peak. A broad carbon peak also exists in this spectra which is associated with the amorphous surface passivation, whose peak signal is within a factor of 2 of the peak arising from the porous silicon.

To test the robustness of the carbonization process, pillars were formed into the PS under a propane flow of 600 sccm, with dwell times Δt doubling for each pillar up to an exposure time of 205 s, and repeated for optical powers (P) of 6 mW, 1.5 mW, 0.38 mW and 94 μW. Subsequently, the films were immersed in AZ326 developer containing in 1% KOH, typically used during microelectronics processing of positive photoresists. The ability to survive such chemical immersions is an important test of the robustness of the passivation. [16], [9] Immersion in KOH stripped the unpassivated PS from the surface leaving bare silicon and laser written features. At low powers and short dwell times, pillars did not remain after immersion but a discoloration of the substrate was observed indicating the remnants of the features formed at the upper PS layer. We believe the determination of whether features would detach or not depends on the effective thermal conductivity (K_{eff}) of the films, which increased as the depth of the carbonisation approached the substrate. The steady state temperature depends on[27] $P\sqrt{\Delta t/K_{eff}}$ so that an increase in time and/or power is required to reach the required passivation temperature of 600 °C in the region nearer the substrate. **Figure 5** shows two cases of the minimum conditions required to create a pillar attached to the substrate after KOH immersion, where in each case the condition $P\sqrt{\Delta t} = 3.8\, mW.s^{0.5}$ was the same. Below this combination of time and power, no pillars were formed, while above, pillars consistently formed. From the 3D data in Figure 5a and Figure 5b, we can see significant damage to the underlying PS/Si-substrate interface caused by this combination of power and dwell time. Profile

Author Manuscript

This article is protected by copyright. All rights reserved.

data in Figure 5c indicates straight side walls were obtained with evidence of mass transport at the top edges of the pillar due to the high temperatures achieved.

The results obtained in this work indicate that carbonized porous regions can be created along side oxidized features by modulation of the gas flow during laser writing. Subsequent wet processing using HF immersion provides a simple method to define the passivated carbonized features as shown in Figure 3. The carbonized PS is expected to have a larger Young's modulus than as-fabricated PS, relatively unchanged optical characteristics and good electrical properties.[16] All these properties are important for the fabrication of free-standing, electrically-actuated MEMS sensors which require strong, thin films patterned to contain microscale features which enable them to be insensitive to inertial (gravitational) effects.[28] Using a combination of multilayer optical films defined during anodization,[29] laser defined lateral features and suspended thin films,[15] we believe complex technologies such as MEMS microspectrometers[30] (FTIR on a chip) could be created using this process. The large surface area associated with the open-pores of the patterned carbonized features offers the possibility for very high sensitivity detection of a range of gas and liquid analytes in the infrared using this approach. The tensile stress in our carbonized porous films is advantageous for suspended microbeams, as compressive stress associated with oxides leads to beam buckling which is unacceptable in optical MEMS sensors.

4. Conclusions

We have investigated the formation of laser written features into porous silicon, creating both oxidized porous silicon and carbonized porous silicon. We have demonstrated the use of propane as an appropriate gas during laser writing to form selective carbonized regions with feature widths

Author Manuscript

This article is protected by copyright. All rights reserved.

down to 1.8 µm. Complex features with films containing porous silicon, oxidized porous silicon and carbonized porous silicon can all be achieved within the same sample by switching gas flow during laser writing. Once carbonized regions are formed, they can be overwritten with an air-passivation step to convert the surrounding region into oxidized porous silicon. We found that both oxidized and carbonized features could be formed through the entire film thickness of the 2.5 µm porous silicon film where sufficient power or exposure time was used. Laser induced carbonization of porous silicon allows positive features to be formed where exposed, compared with the removal of HF-etched oxidized regions which results in negative features where exposed to the laser beam. This work significantly enhances the ability to selectively control the material's properties. By controlling nanoscale pore size and porosity during anodization and selectively passivating lateral features at the microscale with our laser writing approach which maintains the integrity of the pores, the composition of these porous films can be engineered from micrometer to the nanometer scales.

Author Manuscript

Acknowledgements

This work has been supported by the Australian Research Council under DP170104266. The authors acknowledge the facilities, and the scientific and technical assistance of the Australian National Fabrication Facility at the Centre for Microscopy, Characterisation & Analysis, The University of Western Australia, a facility funded by the University, State and Commonwealth Governments.

References

This article is protected by copyright. All rights reserved.

[1] Y.-L. Khung, S. D. Graney, N. H. Voelcker, *Biotechnology Progress* Micropatterning of Porous Silicon Films by Direct Laser Writing **2006**, *22*, 1388.

[2] A. M. Ruminski, G. Barillaro, E. Secret, W. D. Huang, A. Potocny, U. Carion, C. Wertans, M. J. Sailor, *Advanced Optical Materials* Topological Control of Porous Silicon Photonic Crystals by Microcontact Printing **2013**, *1*, 510; M. Lai, G. M. Sridharan, G. Parish, S. Bhattacharya, A. Keating, *Nanoscale Research Letters* Multilayer porous silicon diffraction gratings operating in the infrared **2012**, *7*, 645.

[3] J. D. Ryckman, M. Liscidini, J. E. Sipe, S. M. Weiss, *Nano Letters* Direct Imprinting of Porous Substrates: A Rapid and Low-Cost Approach for Patterning Porous Nanomaterials **2011**, *11*, 1857.

[4] A. Jane, R. Dronov, A. Hodges, N. H. Voelcker, *Trends in Biotechnology* Porous silicon biosensors on the advance **2009**, *27*, 230.

[5] K. Kim, T. E. Murphy, *Opt. Express* Porous silicon integrated Mach-Zehnder interferometer waveguide for biological and chemical sensing **2013**, *21*, 19488.

[6] T. D. James, G. Parish, C. A. Musca, A. J. Keating, *Electrochemical and Solid-State Letters* N2-Based Thermal Passivation of Porous Silicon to Achieve Long-Term Optical Stability **2010**, *13*, H428.

[7] J. Riikonen, M. Salomäki, J. van Wonderen, M. Kemell, W. Xu, O. Korhonen, M. Ritala, F. MacMillan, J. Salonen, V.-P. Lehto, *Langmuir* Surface Chemistry, Reactivity, and Pore Structure of Porous Silicon Oxidized by Various Methods **2012**, *28*, 10573.

[8] J. Salonen, M. Björkqvist, E. Laine, L. Niinistö, *Applied Surface Science* Stabilization of porous silicon surface by thermal decomposition of acetylene **2004**, *225*, 389.

[9] M. Lai, G. Parish, Y. Liu, J. M. Dell, A. J. Keating, *Journal of Microelectromechanical Systems* Development of an Alkaline-Compatible Porous-Silicon Photolithographic Process **2011**, *20*, 418.

[10] Z. M. Rittersma, W. J. Zaagman, M. Zetstra, W. Benecke, *Smart Materials and Structures* A monitoring instrument with capacitive porous silicon humidity sensors **2000**, *9*, 351; K. Seong-Jeen, P. Jae-Yoon, L. Sang-Hoon, Y. Seung-Hwan, *Journal of Physics D: Applied Physics* Humidity sensors using porous silicon layer with mesa structure **2000**, *33*, 1781.

[11] R. Caroselli, S. Ponce-Alcántara, F. P. Quilez, D. M. Sánchez, L. T. Morán, A. G. Barres, L. Bellieres, H. Bandarenka, K. Girel, V. Bondarenko, J. García-Rupérez, *Opt. Express* Experimental study of the sensitivity of a porous silicon ring resonator sensor using continuous in-flow measurements **2017**, *25*, 31651.

Author Manuscript

This article is protected by copyright. All rights reserved.

[12] I. Rea, M. Iodice, G. Coppola, I. Rendina, A. Marino, L. De Stefano, *Sensors and Actuators B: Chemical* A porous silicon-based Bragg grating waveguide sensor for chemical monitoring **2009**, *139*, 39.

[13] A. M. Rossi, G. Amato, V. Camarchia, L. Boarino, S. Borini, *Applied Physics Letters* High-quality porous-silicon buried waveguides **2001**, *78*, 3003.

[14] C. Populaire, B. Remaki, V. Lysenko, D. Barbier, *Applied Physics Letters* On mechanical properties of nanostructured meso-porous silicon **2003**, *83*, 1370; A. M. Rossi, S. Borini, L. Boarino, G. Amato, *physica status solidi (a)* Lateral structuring of porous silicon: application to waveguides **2003**, *197*, 284.

[15] X. Sun, A. Keating, G. Parish, *Microporous and Mesoporous Materials* Stress control of porous silicon films for microelectromechanical systems **2015**, *218*, 88.

[16] J. Salonen, E. Mäkilä, *Advanced Materials* Thermally Carbonized Porous Silicon and Its Recent Applications **2018**, *30*, 1703819.

[17] J. P. Li, A. J. Steckl, *Journal of The Electrochemical Society* Nucleation and Void Formation Mechanisms in SiC Thin Film Growth on Si by Carbonization **1995**, *142*, 634.

[18] A. J. Steckl, J. P. Li, *IEEE Transactions on Electron Devices* Epitaxial growth of β-SiC on Si by RTCVD with C_3H_8 and SiH_4 **1992**, *39*, 64.

[19] J. Lin, Z. Peng, Y. Liu, F. Ruiz-Zepeda, R. Ye, E. L. G. Samuel, M. J. Yacaman, B. I. Yakobson, J. M. Tour, *Nature Communications* Laser-induced porous graphene films from commercial polymers **2014**, *5*, 5714.

[20] R. Rahimi, M. Ochoa, B. Ziaie, *ACS Applied Materials & Interfaces* Direct Laser Writing of Porous-Carbon/Silver Nanocomposite for Flexible Electronics **2016**, *8*, 16907.

[21] S. Luo, P. T. Hoang, T. Liu, *Carbon* Direct laser writing for creating porous graphitic structures and their use for flexible and highly sensitive sensor and sensor arrays **2016**, *96*, 522.

[22] J. B. In, B. Hsia, J.-H. Yoo, S. Hyun, C. Carraro, R. Maboudian, C. P. Grigoropoulos, *Carbon* Facile fabrication of flexible all solid-state micro-supercapacitor by direct laser writing of porous carbon in polyimide **2015**, *83*, 144.

[23] C. Liu, Y. Liao, F. He, Y. Shen, D. Chen, Y. Cheng, Z. Xu, K. Sugioka, K. Midorikawa, *Opt. Express* Fabrication of three-dimensional microfluidic channels inside glass using nanosecond laser direct writing **2012**, *20*, 4291.

Author Manuscript

This article is protected by copyright. All rights reserved.

[24] S. Luca De, R. Ilaria, M. A. Nigro, G. D. C. Francesco, R. Ivo, *Journal of Physics: Condensed Matter* A parametric study of laser induced ablation–oxidation on porous silicon surfaces **2008**, *20*, 265009.

[25] M. Lax, *Journal of Applied Physics* Temperature rise induced by a laser beam **1977**, *48*, 3919; E. Abraham, J. M. Halley, *Applied Physics A* Some calculations of temperature profiles in thin films with laser heating **1987**, *42*, 279.

[26] J. Salonen, M. Björkqvist, J. Paski, *Sensors and Actuators A: Physical* Temperature-dependent electrical conductivity in thermally carbonized porous silicon **2004**, *116*, 438.

[27] S. Alimpiev, S. Nikiforov, V. Karavanskii, T. Minton, J. Sunner, *Journal of Chemical Physics* On the mechanism of laser-induced desorption-ionization of organic compounds from etched silicon and carbon surfaces **2001**, *115*, 1891.

[28] M. J. Madou, *Fundamentals of Microfabrication: The Science of Miniaturization, Second Edition*, Taylor & Francis, 2002.

[29] M. J. Sailor, *Porous Silicon in Practice: Preparation, Characterization and Applications*, Wiley-VCH, 2012.

[30] G. Lammel, S. Schweizer, P. Renaud, *Optical Microscanners and Microspectrometers using Thermal Bimorph Actuators*, Springer US, 2013; J. Antoszewski, K. J. Winchester, T. Nguyen, A. J. Keating, K. K. M. B. D. Silva, C. A. Musca, J. M. Dell, L. Faraone, *IEEE Journal of Selected Topics in Quantum Electronics* Materials and Processes for MEMS-Based Infrared Microspectrometer Integrated on HgCdTe Detector **2008**, *14*, 1031.

Table 1. A comparison of laser writing approaches involving porous materials based on polymers and silicon. Shaded row indicates this work.

Material	Passivation	Size	Device	Pores	Gas
[20] polyimide	porous+carbonized	200 μm	conductive traces	filled with nanoparticles	air
[21] polyimide	porous+carbonized	100 μm	strain gage	open	air
[22] polyimide	porous+carbonized	10 μm	supercapacitors	open	air

Author Manuscript

This article is protected by copyright. All rights reserved.

[23] porous SiO_2	------	20 µm	microfluidic	closed	N_2
[1] oxidized PS	ablated	40 µm	cell growth	------	air
[12] PS		3 µm	guide/grating	closed	air
[5, 13] PS	oxidized	2-3 µm	waveguide	open (HF dip)	air
[24] PS	oxidized	1 µm	none (study)	open & closed	air
PS (this work)	oxidized & carbonized	1.8 µm	none (study)	open	air/ C_3H_8

Manuscript

Figure 1

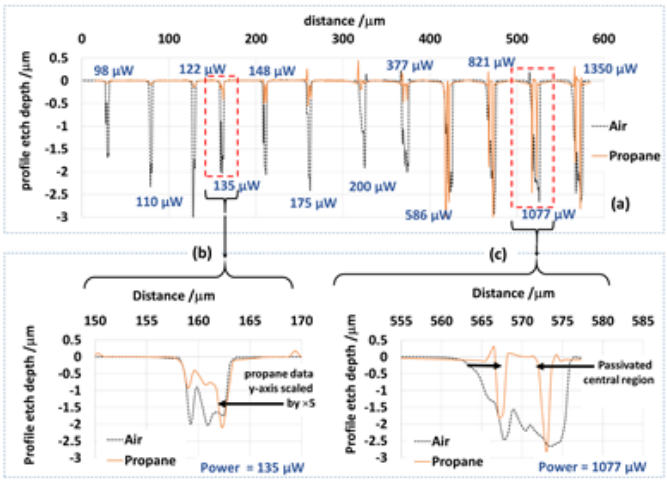

Figure 1: (a) Measured profile after HF-immersion using a range of optical powers in air (dotted line) and propane (solid line); fine detail shown for (b) 135 µW and (c) 1077 µW, for a 2.5-µm thick porous silicon film after exposure to air and propane (600 sccm). Note the scale change in (b) to highlight features from the propane exposure. In all cases, the laser beam diameter was ∅ = 3µm and the raster speed of the beam was v = 200 µm/s

This article is protected by copyright. All rights reserved.

Figure 2

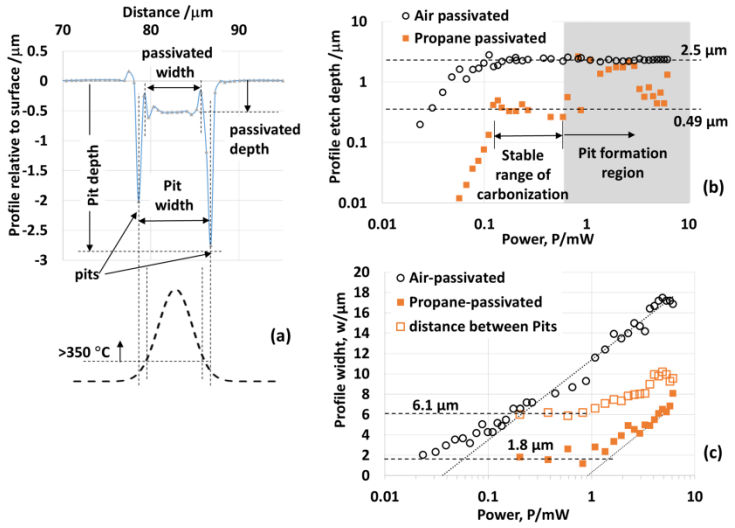

Figure 2: Measured profile characteristics after HF immersion of laser written samples using a beam diameter ∅ = 3µm and velocity v = 200 µm/s. (a) Profile of feature written sample in propane, defining depths and widths of passivated and pit regions; (b) variation in the etched profile depth with optical power for the air and propane-passivated features of porous silicon; (c) variation of etch profile width for air and propane-passivated features as well as the width of the pit defined in (a). In (c) the dashed lines indicate the pit and propane-passivated width at low powers while the dotted lines indicate linear extrapolation (on semi-log) at high powers.

Author Manuscript

This article is protected by copyright. All rights reserved.

Figure 3

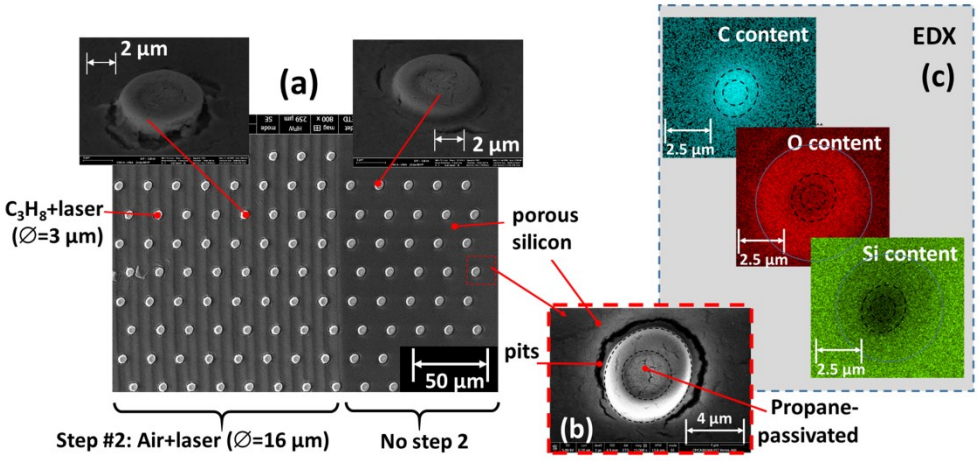

Figure 3: Two step exposure to form carbonized pillars of PS: Step #1: P = 0.83 mW (∅ = 3µm, v = 0 µm/s) in C_3H_8 (600 sccm) and Step #2: P = 6 mW (∅ =16 µm, v = 50 µm/s) in air. (a) SEM image after HF immersion of a sample with single point exposure written into porous silicon in Step #1, followed by Step #2 applied to a portion of the film. Insets show angled view of the pillars in each region; (b) expanded view of a porous pillar showing cracking around the pillar in the region which had not undergone Step #2; (c) EDX measurements of carbon, oxygen and silicon content on the image in (b).

Author Manuscript

This article is protected by copyright. All rights reserved.

Figure 4

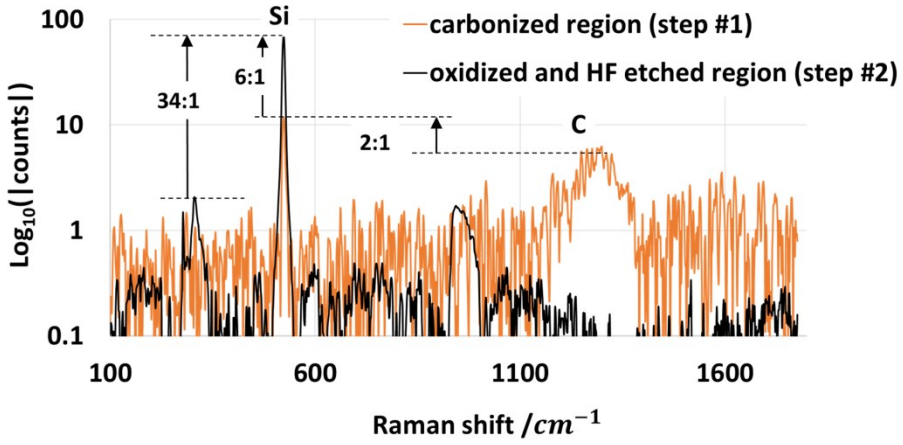

Figure 4: Raman spectra taken from the carbonized porous silicon associated with Step #1 in Figure 3, and corresponding Raman spectra from the oxidized and HF-immersed region associated with Step #2 in Figure 3.

Figure 5

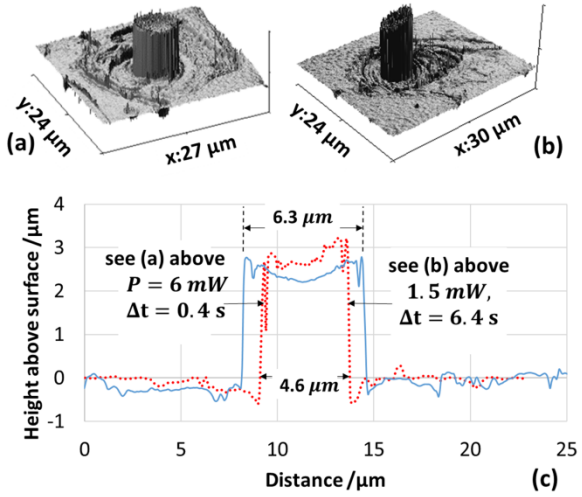

Figure 5: 3D image profiles formed under propane flow and subsequently dipped into 1% KOH solution. The minimum conditions required for pillars to be attached to the substrate were (a)

This article is protected by copyright. All rights reserved.

power P = 6 mW, dwell time 0.4 s; (b) power P=1.5 mW, dwell time 6.4 s; (c) sectional profile of each pillar. Measurement performed with a beam width of ∅ = 3 µm.

Manuscript

Table of Contents Graphic (55 mm broad × 50 mm high) SCALED

TOC Graphic
55 mm broad ×
50 mm high
SCALED

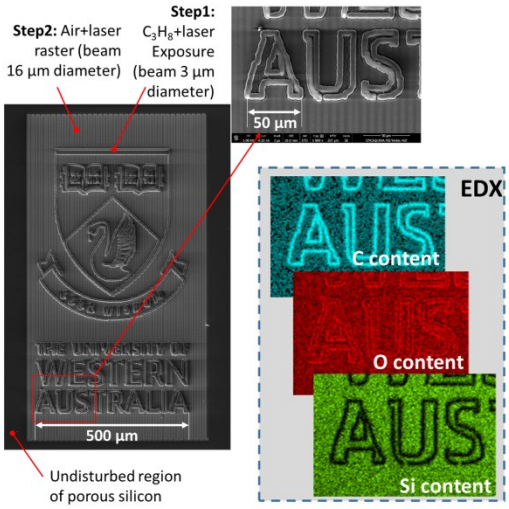

A laser written carbonized porous silicon pattern of the University of Western Australia crest. In Step #1 a 405-nm laser of beam diameter 3 µm passivates the porous film under C_3H_8 flow, while in Step #2 a larger 16 µm beam oxidizes the film in air. SEM and EDX data measured after HF immersion to remove the oxide.

Author Manuscript

This article is protected by copyright. All rights reserved.